

# High Energy Neutrinos from Gamma-Ray Bursts with Precursor Supernovae

Soebur Razzaque,<sup>1</sup> Peter Mészáros<sup>1</sup> and Eli Waxman<sup>2</sup>

<sup>1</sup>*Department of Astronomy & Astrophysics, Department of Physics,  
Pennsylvania State University, University Park, Pennsylvania 16802, USA*

<sup>2</sup>*Department of Condensed Matter Physics, Weizmann Institute of Science, Rehovot 76100, Israel*

(Dated: October 24, 2018)

The high energy neutrino signature from proton-proton and photo-meson interactions in a supernova remnant shell ejected prior to a gamma-ray burst provides a test for the precursor supernova, or supranova, model of gamma-ray bursts. Protons in the supernova remnant shell, and photons entrapped from a supernova explosion or a pulsar wind from a fast-rotating neutron star remnant provide ample targets for protons escaping the internal shocks of the gamma-ray burst to interact and produce high energy neutrinos. We calculate the expected neutrino fluxes, which can be detected by current and future experiments.

PACS numbers: 96.40.Tv, 98.70.Rz, 98.70.Sa

Gamma-ray bursts (GRBs) are thought to be possible sources of high energy neutrinos. In the currently favored models the  $\gamma$ -ray emission is attributed to radiation from shock-accelerated electrons in the relativistic fireball outflow or jet from a cataclysmic stellar event. The latter may be connected to compact stellar mergers, or the core collapse of a massive stellar progenitor (collapsar), which could also involve a core-collapse supernova (SN) [1]. Together with electrons, the shocks are expected to accelerate protons as well, and high energy neutrinos are thought to be produced dominantly by  $p\gamma$  interactions of the protons with synchrotron or inverse Compton scattered photons [2, 3]. Recent reports of detection of X-ray lines from several GRB afterglows have been interpreted [4], although not unambiguously, as providing support for a version of the collapsar model in which a SN explosion occurs weeks before the GRB (the ‘‘supranova’’ model, [5]). In the supranova scenario the supernova remnant (SNR) shell provides nucleon targets for  $pp$  interactions with protons accelerated in the MHD wind of a pre-GRB pulsar [6], leading to a 10 TeV neutrino precursor to the GRB (other nucleon targets from a stellar companion disruption leading to  $\pi^0$  decay GeV  $\gamma$ -rays were discussed by [7]). The SNR also provides additional target photons for  $p\gamma$  interactions [6] with internal shock-accelerated protons, resulting in  $\sim 10^{16}$  eV neutrinos. In this Letter we investigate some important unexplored aspects of the GRB-SNR interaction, namely  $pp$  and  $p\gamma$  interactions involving GRB protons in the shocked shell, which have significant consequences in the assessment of the neutrino signatures from these objects.

*SNR target nucleons and photons.* — The typical mass ejected in a SN is  $M_{\text{SNR}} \sim m_{\text{SNR}} M_{\odot} = 2 \times 10^{33} m_{\text{SNR}} \text{ g}$ . For a nominal sub-relativistic shell speed  $v = 10^9 \text{ cm/s}$ , the typical distance reached is  $R_{\text{SNR}} \sim 10^{14} v_9 t_d \text{ cm}$  in  $t_d$  days. We assume that the gas is roughly isotropically ejected in a shell of width  $\delta = \Delta R/R = 0.1 \delta_{-1}$  and average column density  $\Sigma \approx 1.6 \times 10^4 m_{\text{SNR}} v_9^{-2} t_d^{-2} \text{ g-cm}^{-2}$ .

The deposition of  $10^{51} E_{51}$  ergs in a SN progeni-

tor stellar envelope of dimension  $R_* = 10^{12} R_{12} \text{ cm}$  heats it to a temperature  $T_o \sim 1 E_{51}^{1/4} R_{12}^{-3/4} \delta_{-1}^{-1/4} \text{ keV}$ . The mean photon energy in the SNR shell is  $\epsilon_{\gamma, \text{SN}} \sim 20 E_{51}^{1/4} \delta_{-1}^{1/3} R_{12}^{1/4} v_9^{-1} t_d^{-1} \text{ eV}$ . The photon column density in the SNR is  $\Sigma_{\gamma, \text{SN}} \sim 3 \times 10^{32} E_{51}^{3/4} \delta_{-1}^{1/3} R_{12}^{-1/4} v_9^{-1} t_d^{-1} \text{ cm}^{-2}$ . The  $p\gamma$  optical depth and threshold proton energy at the  $\Delta$ -resonance are

$$\begin{aligned} \tau_{p\gamma, \text{SN}} &\sim 3 \times 10^4 E_{51}^{3/4} \delta_{-1}^{1/3} R_{12}^{-1/4} v_9^{-1} t_d^{-1} \\ E_{p, \text{th, SN}} &\sim 10^7 E_{51}^{-1/4} \delta_{-1}^{-1/3} R_{12}^{-1/4} v_9 t_d \text{ GeV}. \end{aligned} \quad (1)$$

The collapse of the Fe core can lead initially to a fast-rotating pulsar of rotational energy  $E_{\text{rot}} \sim 10^{53} \text{ erg}$  and spin-down time  $\sim 3 \times 10^6 \text{ s}$  [6, 8], emitting an MHD wind of luminosity  $L_m \sim 10^{46} L_{m46} \text{ erg/s}$ . Besides ejecting the SNR envelope, the SN explosion may leave behind parts of the He core, which take longer in falling back to make a black hole leading to the GRB (months in the supranova scenario). If the fall-back is anisotropic and a channel forms in the He core (e.g. along the rotation axis), the relativistic MHD wind may flow out and impact the SNR shell further out. The MHD wind is highly relativistic, and is decelerated to a subrelativistic velocity in a reverse shock, driving a forward shock into the shell [9]. The shock velocity  $v_s$  in the observer frame satisfies, from pressure balance in the shock frame,  $v_s - v \simeq [L_m(10^{-1} R/c)/M_{\text{SNR}}]^{1/2} \simeq 10^{-1} [E(t)/M_{\text{SNR}}]^{1/2} \sim 10^{-2} c$  for typical  $E(t) = t L_m$  and  $M_{\text{SNR}}$ . Thus the shock will propagate through a significant fraction of the shell width, and we approximate the situation by taking the shock to cross the entire shell, producing photons distributed throughout the shell. Given the high Thomson optical depth in the SNR shell, these photons thermalize to a maximum energy  $\epsilon_{\gamma, m} \sim 0.1 L_{m46}^{1/4} \delta_{-1}^{1/4} v_9^{-3/4} t_d^{-1/2} \text{ keV}$ , assuming that all the MHD wind energy goes into photons. The  $p\gamma$  optical depth and threshold proton energy at  $\Delta$  production, are

$$\tau_{p\gamma, m} \sim 3 \times 10^4 L_{m46}^{3/4} \delta_{-1}^{1/4} v_9^{-1/2} t_d^{-1/2}$$

$$E_{p,\text{th,m}} \sim 2 \times 10^6 L_{46}^{1/4} \delta_{-1}^{-1/4} v_9^{-3/4} t_d^{-1/2} \text{ GeV}. \quad (2)$$

Additional target photons may arise from parts of the disrupted He core, no longer in hydrostatic equilibrium and moving outwards inside the shell. However, even if they have super-Eddington luminosities  $L_{*,\text{He}} \sim 10^{44}$  erg/s as inferred in some SN, these photons have an optical depth  $\tau_{p\gamma} \sim 5L_{44}v_9^{-2}t_d^{-1}$  for protons with  $E_p \gtrsim 3 \times 10^8 t_d$  GeV, negligible compared to Eqs. (1) and (2).

The non-relativistic MHD forward shock moving into the SNR is likely to be collisionless (as also generally assumed for non-relativistic GRB internal shocks [10]). The transition is dominated by the process giving the narrower shock width, i.e. the shortest timescales for changing particle momenta. A collisionless shock thickness is  $\sim c/(\beta\omega_p)$ , where  $\beta$  is shock velocity,  $\omega_p$  is plasma ion frequency. For our parameters  $\sim 1 M_\odot$  shell at  $\sim 10^{14}$  cm radius,  $\omega_p = 3 \times 10^{10}$ /sec and  $\beta = 0.01$ , this shock width is 100 cm. The thickness of a radiation shock is  $l/\beta$ , where  $l$  is the photon mean free path, giving a thickness  $\sim 10^{11}$  cm. The thickness for  $pp$  collisions is even larger due to a smaller cross section than Thomson. This strongly suggests that the shock is collisionless.

The average magnetic field inside the SNR shell is

$$B \sim 10^4 \xi_B^{1/2} m_{\text{snr}}^{1/2} \delta_{-1}^{-1/2} v_9^{-1/2} t_d^{-3/2} \text{ G}, \quad (3)$$

where  $\xi_B$  is the equipartition value in respect to the proton kinetic energy. Equating the acceleration time  $t_a \sim 2\pi Amc\gamma/(\beta^2 eB)$  [where  $\beta = (v_s - v)/c \sim 10^{-2}\beta_{-2}$  is the relative shock speed in the shell, and  $A \sim 10A_1$ ] to the synchrotron loss time  $t_{\text{sy}} = 3m^3 c^5/(2e^4 B^2 \gamma)$ , the maximum accelerated particle Lorentz factor is  $\gamma_{\text{mx}} = 2 \times 10^{10} A_1^{-1/2} (m/m_p) B^{-1/2}$ . For the field of Eq. (3), the maximum proton Lorentz factor is  $\gamma_{p,\text{mx}} \sim 2 \times 10^7 A_1^{-1/2} \beta_{-2}^{-1/4} \xi_B^{-1/4} m_{\text{snr}}^{-1/4} \delta_{-1}^{1/4} v_9^{1/4} t_d^{3/4}$ . The maximum electron Lorentz factor is  $m_e/m_p$  lower and the synchrotron photon peak energy is  $\omega_{\text{sy}} \approx 0.2 A_1^{-1} \beta_{-2}^2$  keV, but due to the high Thomson depth these photons are thermalized to the blackbody value  $\epsilon_{\gamma,\text{m}} \sim 0.1$  keV.

*GRB protons and interactions in the SNR.*— The GRB isotropic-equivalent  $\gamma$ -ray luminosity is  $L_\gamma^{\text{iso}} \approx 10^{52} L_{52}$  ergs/s. The corresponding GRB total proton luminosity is  $dN_p/dt = L_\gamma/\Gamma m_p c^2 = 2 \times 10^{52} L_{52} \Gamma_{300}^{-1} \text{ s}^{-1}$ . Assuming that a fraction  $\xi_p \lesssim 1$  of these is accelerated in the internal shocks results in a proton distribution  $d^2 N_p/dE_p dt \simeq 6 \times 10^{54} L_{52} \xi_p E_{p,\text{GeV}}^{-2} \text{ GeV}^{-1} \text{ s}^{-1}$ . High energy protons interact with synchrotron and inverse Compton scattered photons in the GRB fireball shock dominantly through  $p\gamma \rightarrow \Delta \rightarrow n\pi^+/p\pi^0$  [2], resulting in  $\gtrsim 100$  TeV neutrinos. The cross-section for  $\Delta$  production at threshold  $E_p E_\gamma \sim 0.2 \Gamma^2 \text{ GeV}^2$  in the observer frame is  $\sim 0.1$  mb. The optical depth for  $E_p > 10^7$  GeV is  $\tau_{p\gamma} \gtrsim 1$  in the high  $\sim$  MeV photon density in the internal shocks. Since protons lose  $\sim 20\%$  of their energy per interaction, each proton will undergo a couple of interactions, thus roughly half of the protons with

$E_p > 10^{16}$  eV will be converted to neutrons and escape. At lower energies, protons may be prevented by fireball magnetic field from escaping to the SNR. However, since internal shock radii range over  $3 \times 10^{12} - 3 \times 10^{14}$  cm, this may allow a significant fraction of  $\lesssim 10^{16}$  eV protons to interact with the SNR shell. This implies that a fraction  $\eta_p(E_p) \lesssim 1$  of protons escape the fireball shock region to propagate outwards. The isotropic-equivalent observer-frame proton luminosity impacting the shell is

$$\frac{d^2 N_p}{dE_p dt} = 6 \times 10^{54} E_{p,\text{GeV}}^{-2} L_{52} \xi_p \eta_p(E_p) \text{ GeV}^{-1} \text{ s}^{-1}. \quad (4)$$

The large  $p\gamma$  optical depths for both the SN-shock  $\epsilon_{\text{sn}}$  and the pulsar MHD wind shock  $\epsilon_{\text{m}}$  photons [Eqs. (1) and (2)] trapped inside the SNR shell causes most of the incoming protons above the thresholds [Eqs. (1) and (2)] to undergo photomeson production. Low energy protons below  $\Delta$  production threshold may interact with SNR protons. If  $\xi_{\text{sh}}$  (typically  $\lesssim 10^{-1}$ ) is the fraction of shell protons which is accelerated to relativistic energies by the collisionless MHD shock going through the SNR shell, the column density of cold protons in the SNR shell is  $\Sigma_p \sim 10^{28} \zeta_{\text{sh}} m_{\text{snr}} v_9^{-2} t_d^{-2} \text{ cm}^{-2}$ , where  $\zeta_{\text{sh}} = 1 - \xi_{\text{sh}} \sim 1$ .

The total cross-section for  $pp$  interaction has been measured up to very high energies (120 mb at  $\sqrt{s} = 30$  TeV [11]) in accelerator experiments. We take the mean  $pp$  cross-section to be  $\langle \sigma_{pp} \rangle \approx 100$  mb in the TeV and above energy range. The corresponding mean optical depth is

$$\langle \tau_{pp} \rangle = \Sigma \langle \sigma_{pp} \rangle \approx 10^3 \zeta_{\text{sh}} m_{\text{snr}} v_9^{-2} t_d^{-2}. \quad (5)$$

To calculate the neutrino flux from  $pp$  interactions, one needs to know the secondary charged particle multiplicities as a function of  $\sqrt{s}$ . Analytic calculations of this multiplicity, known as the KNO scaling law [12], are based on the rapidity ( $y = \ln[(E+p_z)/(E-p_z)]/2$ , taking the beam direction along the  $z$ -axis) distribution of the secondary charged particles. Analytically the total charged particle multiplicity increases as  $\sim \ln(s)$ . Accelerator data show a slightly faster growth in  $pp$  interactions measured up to  $\sqrt{s} = 1.8$  TeV [13]. An extrapolation up to  $\sqrt{s} \sim 400$  TeV, relevant for our calculation, for  $\pi^\pm$  and  $K^\pm$  multiplicities from  $pp$  interactions using  $\sim \ln(s)$  scaling is certainly very conservative. There exist in the literature other faster growing models such as  $\sim s^{0.3}$  [14]. The dominant neutrino production channels in our calculation are  $pp \rightarrow \pi^\pm/K^\pm \rightarrow \mu\nu_\mu \rightarrow e\nu_e\nu_\mu\bar{\nu}_\mu$ . High energy photons are also produced from  $\pi^0 \rightarrow \gamma\gamma$ .

We used the PYTHIA 6.2 event generator [15] to simulate  $pp$  interactions [16]. The angular deviation of a secondary particle is related to its Lorentz invariant rapidity ( $y$ ) as  $\theta \approx 1/\cosh(y)$ . We select  $\pi^\pm$  and  $K^\pm$  which are forward, namely,  $y \geq 0$ . The average  $\pi^\pm$  and  $K^\pm$  multiplicities measured at  $\sqrt{s} = 540$  GeV in the pseudo-rapidity ( $\eta \approx y$  for momentum  $p \gg m$ ) region  $0 \leq \eta \leq 5$  are  $\langle n_\pi \rangle = 11.15$  and  $\langle n_K \rangle = 1.25$  [13]. These numbers

agree with our PYTHIA simulations within error bars. For  $y \geq 0$  we have  $\langle n_\pi \rangle = 15.3$  and  $\langle n_K \rangle = 1.7$  at  $\sqrt{s} = 540$  GeV from simulations. At the highest energy,  $E_p = 10^{20}$  eV ( $\sqrt{s} = 4.33 \times 10^5$  GeV),  $\ln(\sqrt{s})$  extrapolation gives  $\langle n_\pi \rangle = 15.3 \times \ln(4.33 \times 10^5/540) \approx 103$ , about 75% of our simulated value of 136. Similarly  $\langle n_K \rangle = 1.7 \times \ln(4.33 \times 10^5/540) \approx 11.4$ , also about 75% of our simulated value of 15.2 at  $E_p = 10^{20}$  eV. For our calculation we used more conservative values:  $\langle n_\pi \rangle = 103$  and  $\langle n_K \rangle = 11.4$  at  $E_p = 10^{20}$  eV and  $\ln(\sqrt{s})$  scaling at lower energies.

Secondary charged particles ( $\pi^\pm$  and  $K^\pm$ ) in the  $pp$  interaction follow a  $1/E$  energy distribution [16]. The energy of a particle of mass  $m$  ranges from  $m \cosh(y)\gamma_{\text{cm}}$ , where  $\gamma_{\text{cm}}$  is the Lorentz boost of the center of mass in the lab frame and  $\cosh(y)$  is the rapidity dependent boost factor, up to the primary proton energy  $E_p$ . For  $y \geq 0$  we use for secondary  $\pi^\pm$  and  $K^\pm$  the range

$$\gamma_{\text{cm}} m_{\pi, K} \leq E_{\pi, K} \lesssim E_p. \quad (6)$$

The pions and kaons decay into neutrinos with Lorentz-expanded decay times ( $\tau_{\pi, K} \gamma_{\pi, K}$ ) in the observer frame.

In the  $\pi^\pm/K^\pm \rightarrow e\nu_e \nu_\mu \bar{\nu}_\mu$  decay the  $e$  and 3  $\nu$ 's each share roughly 1/4 of the pion/kaon energy. The branching ratio for the kaon decay channel is  $\sim 64\%$ . The  $\nu$  multiplicity for an incident proton of energy  $E_p \leq 10^{11}$  GeV, using Eq. (6), is then

$$M_\nu(E_p) = \frac{1}{4} \mathcal{N}_{\pi, K} \left( \frac{E_\nu}{\text{GeV}} \right)^{-1} \left[ \frac{1}{2} \ln \left( \frac{10^{11} \text{ GeV}}{E_p} \right) \right]^{-1} \times \Theta \left( \frac{1}{4} \frac{m_{\pi, K}}{\text{GeV}} \gamma_{\text{cm}} \leq \frac{E_\nu}{\text{GeV}} \leq \frac{1}{4} \frac{E_p}{\text{GeV}} \right) \quad (7)$$

for each type of neutrinos:  $\nu_e$ ,  $\bar{\nu}_\mu$  and  $\nu_\mu$ . Here  $\Theta$  is a step function following from Eq. (6). The normalization factors  $\mathcal{N}_\pi$  and  $\mathcal{N}_K$  are found by integrating the  $1/E$  distribution of  $\pi^\pm$  and  $K^\pm$  in the energy range given in Eq. (6) for  $E_{\pi, K}^{\text{mx}} \approx 10^{11}$  GeV and equating to the respective total numbers,  $\mathcal{N}_\pi = \langle n_\pi \rangle / \ln(E_{\pi, K}^{\text{mx}}/m_\pi \gamma_{\text{cm}}) \approx 7$ ,  $\mathcal{N}_K = 0.64 \langle n_K \rangle / \ln(E_{\pi, K}^{\text{mx}}/m_K \gamma_{\text{cm}}) \approx 0.6$ .

An additional  $pp$  component may result from protons accelerated by the collisionless shock in the shell colliding with shell thermal nucleons. For a typical SNR shell energy  $10^{51} E_{51}$  ergs this neutrino component has  $\lesssim \zeta_{sh} 10^{51} E_{51}$  ergs, at least an order of magnitude below the GRB shock proton component, but it could become important for exceptionally energetic supernova shells.

*Neutrino flux calculation.*— The GRB protons from internal shocks undergo  $pp$  interactions below  $E_{p, \text{th}}$  from Eqs. (1) and (2), and  $p\gamma$  interactions above  $E_{p, \text{th}}$ . The neutrino flux ( $\Phi_\nu = d^2 N / dE_\nu dt$ ) at Earth from a single GRB-SNR at distance  $D$  is

$$\Phi_\nu = \frac{1}{4\pi D^2} \begin{cases} \int f_{pp} M_\nu(E_p) \frac{d^2 N}{dE_p dt} dE_p; & E_p \lesssim E_{p, \text{th}} \\ (f_\pi/4) \frac{d^2 N}{dE_p dt}; & E_p > E_{p, \text{th}} \end{cases} \quad (8)$$

for each  $\nu$  type. Here  $f_{pp} = \min(1, \langle \tau_{pp} \rangle)$  from Eq. (5), and  $f_\pi$  is the fraction of  $E_p$  lost to  $\pi$ 's in  $p\gamma$  interactions [2], which is  $\sim 1$  for an SNR with  $\tau_{p\gamma} \gg 1$ . The synchrotron cooling energy  $E_\nu^s$  is found by equating the decay times ( $\tau_j \gamma_j$  with  $j = \pi, K, \mu$ ) and synchrotron cooling times for  $\pi$ 's,  $K$ 's and  $\mu$ 's. For the magnetic field in Eq. (3) we get the maximum energies as

$$\gamma_j^s \approx 2.3 \times 10^4 m_j^{3/2} \tau_j^{-1/2} \xi_B^{-1/2} m_{\text{snr}}^{-1/2} \delta_{-1}^{1/2} v_9^{1/2} t_d^{3/2} \quad (9)$$

where  $m_j$ 's are in GeV and  $\tau_j$ 's are in s. Taking  $m_{\text{snr}} \sim 10$  and typical age  $t_d \sim 50$  d, the maximum energies from Eq. (9) are  $E_\pi^s \sim 10^{10}$  GeV,  $E_K^s \sim 10^{11}$  GeV and  $E_\mu^s \sim 10^9$  GeV, where we used  $\xi_B \approx 10^{-2} \xi_{-2}$  as in typical GRB fits. The corresponding  $\nu$  steepening break energies are  $\gtrsim 10^9$  GeV. The cooling times for inverse Compton scattering are longer than respective lifetimes in the Klein-Nishina limit for  $t_d \gtrsim 10$  d.

The detection probability for a muon neutrino in an ice detector is  $\mathcal{P} \approx 1.7 \times 10^{-6} (E_\nu/\text{TeV})^\beta$ , where  $\beta = 0.8$  for  $E_\nu < 1$  PeV and  $\beta = 0.36$  for  $E_\nu > 1$  PeV. Multiplying this with the flux of Eq. (8) and the burst duration, a numerical integration gives the expected event rates in a  $\text{km}^2$  detector from a single GRB. The total number of  $\nu_\mu$ -induced upward muon events for a single GRB of luminosity  $10^{52} L_{52}$  ergs/s and burst duration  $\Delta t = 10 \Delta_1$  s at  $D \approx 1.6 \times 10^{28} h_{65}^{-1} [(1+z)/2 - (1+z)^{1/2}/2^{1/2}]$  cm  $\sim 10^{28.2} D_{28.2}$  cm for redshift  $z \sim 1$  is

$$\begin{aligned} N_\mu^{\text{TeV-PeV}} &= 1.1 D_{28.2}^{-2} \Delta_1 \xi_p \eta_p(E) L_{52} \\ N_\mu^{\text{PeV-EeV}} &= 0.06 D_{28.2}^{-2} \Delta_1 \xi_p \eta_p(E) L_{52}. \end{aligned} \quad (10)$$

Here we assumed  $f_{pp} = 1$  and  $f_\pi \sim 1$  for  $m_{\text{snr}} \sim 10$  and  $10 \lesssim t_d \lesssim 100$  days. These single-burst numbers can be  $\sim 10^2$  times larger, e.g. for rare bursts with  $D = 10^{27.5}$  cm and  $\Delta t = 100$  s occurring at rates  $\sim 3 \text{ yr}^{-1}$ .

The diffuse  $\nu$ -flux is obtained from Eq. (8) multiplied by  $\Delta t$  and an observed rate  $\sim 600/4\pi \text{ yr}^{-1} \text{ sr}^{-1}$ . Figure 1 shows the diffuse  $\nu_\mu$  energy flux per decade (same for  $\nu_e$  and  $\bar{\nu}_\mu$ ) from GRB models with pre-ejected SNR shells. We assumed  $\sim 10^{-1}$  of protons escape the fireball shocks to reach the shell, where  $f_{pp} = 1$  and  $E_\nu^s = 10^9$  GeV. The top curve is calculated assuming all the GRBs have a SNR shell. This is an upper limit for maximum  $\nu$ 's through  $pp$  and  $p\gamma$  interactions in the SNR shell. The bottom curve assumes 10% of the GRBs have an SNR shell. Also shown are the diffuse  $\nu$ -fluxes from  $p\gamma$  interactions in the internal shocks of bursts (WB [2], short dashed curve), and in GRB afterglows ([3], short dashed curve), as well as the  $\nu$ -flux obtained from the cosmic ray limits (WB Limit [17], long dashed straight lines). In a  $\text{km}^2$  detector [18], the number of diffuse events assuming 10% of GRBs have SNR shells is  $\sim 6 \text{ yr}^{-1} \text{ sr}^{-1}$  at TeV-PeV, and  $\sim 0.3 \text{ yr}^{-1} \text{ sr}^{-1}$  in the PeV-EeV range.

*Discussion and Implications.*— The single-burst  $\nu$ -fluxes calculated here are predicated on the existence of

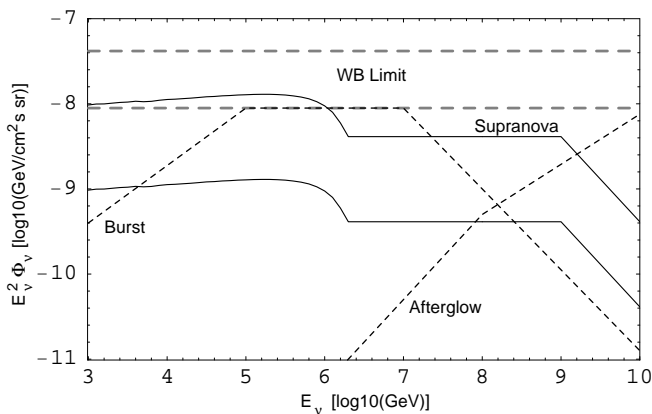


FIG. 1: Diffuse neutrino flux ( $E_\nu^2 \Phi_\nu$ ) from post-supernova (supranova) models of GRBs (solid curves), assuming that (top curve) all GRBs have an SNR shell, or (bottom) 10% of all GRBs have an SNR shell, and  $10^{-1}$  of the fireball protons reach the shells. Long dashed lines correspond to the Waxman-Bahcall cosmic-ray limit, short dashed curves are the diffuse  $\nu$  flux from GRB internal shocks and afterglows.

a pre-ejected SNR shell by the progenitor of the GRB, which occurs at the same location after a delay of weeks [5]. The  $\nu$ 's produced by  $pp$  and  $p\gamma$  interactions between GRB relativistic protons and SNR shell target protons and photons will be contemporary and of similar duration as the GRB electromagnetic event. The high  $pp$  optical depth of the shell also implies a moderately high average Thomson optical depth  $\tau_T \propto t_d^{-2}$  of the shell, dropping below unity after  $\sim 100$  d. Large scale anisotropy as well as clumpiness of the shell will result in a mixture of higher and lower optical depth regions being observable simultaneously, as required in the supranova interpretation of X-ray lines and photon continua in some GRB afterglows [4]. Depending on the fraction of GRB with SNR shells, the contributions of these to the GRB diffuse  $\nu$ -flux has a  $pp$  component which is relatively stronger at TeV-PeV energies than the internal shock  $p\gamma$  component of [2], and a shell  $p\gamma$  component which is a factor 1 (0.1) of the internal shock  $p\gamma$  component (Fig. 1) for a fraction 1 (0.1) of GRB with SNR shells. Due to a higher synchrotron cooling break in the shell, at  $E_\nu \gtrsim 10^{17}$  eV the shell component could compete with the internal [2] and afterglow [3] components.

Our  $pp$  component is caused by internal shock-accelerated power-law protons contemporaneous with the GRB event, differing from [6] who considered quasi-monoenergetic  $\gamma_p \sim 10^{4.5}$  protons from an MHD wind over  $4\pi$  leading to a  $\sim 10$  TeV neutrino months-long precursor of the GRB. Our  $p\gamma$  component arises from the

same GRB-contemporaneous internal shock protons interacting with thermal 0.1 keV photons within the shell wall, whereas [6] consider such protons interacting with photons from the MHD wind inside the shell cavity.

The pre-ejected supernova (supranova) model of GRB is a subject of interest and debate [10] for interpreting the  $\gamma$ - and X-ray data, and independent tests would be useful. The neutrino fluxes discussed here provide such a test, the predicted event rates being detectable with kilometer scale planned Cherenkov detectors.

SR thanks J. P. Ralston for helpful discussions. Work supported by NSF AST0098416.

- 
- [1] S.E. Woosley, *Astrophys. J.* **405**, 273 (1993); B. Paczyński, *Astrophys. J.* **494**, L45 (1998).
  - [2] E. Waxman and J.N. Bahcall, *Phys. Rev. Lett.* **78**, 2292 (1997).
  - [3] E. Waxman and J.N. Bahcall, *Astrophys. J.* **541**, 707 (2000).
  - [4] L. Piro *et al.*, *Science* **290**, 955 (2000); J. Reeves *et al.*, *Nature (London)* **416**, 512 (2002).
  - [5] M. Vietri and L. Stella, *Astrophys. J.* **507**, L45 (1998).
  - [6] D. Guetta and J. Granot, *Phys. Rev. Lett.* **90**, 201103 (2003); J. Granot and D. Guetta, *Phys. Rev. Lett.* **90**, 191102 (2003).
  - [7] J. Katz, *Astrophys. J.* **432**, L27 (1994).
  - [8] J.P. Ostriker and J.E. Gunn, *Astrophys. J.* **164**, L95 (1969); J.E. Gunn and J.P. Ostriker, *Astrophys. J.* **165**, 523 (1971); C. Max and F. Perkins, *Phys. Rev. Lett.* **27**, 1342 (1971).
  - [9] C.F. Kennel and F.V. Coroniti, *Astrophys. J.* **283**, 694 (1984); Y. Gallant and J. Arons, *Astrophys. J.* **435**, 230 (1994); J. Arons and M. Tavani, *Astrophys. J. Suppl. Ser.* **90**, 797 (1996).
  - [10] P. Mészáros, *Annu. Rev. Astron. Astrophys.* **40**, 137 (2002).
  - [11] K. Hagiwara *et al.*, *Phys. Rev. D* **66**, 010001 (2002).
  - [12] Z. Koba *et al.*, *Nucl. Phys.* **B40**, 317 (1972).
  - [13] UA5 Collaboration, G.J. Alner *et al.*, *Phys. Lett.* **160B**, 193 (1985); E735 Collaboration, C.S. Lindsey *et al.*, *Nucl. Phys.* **A544**, 343 (1992).
  - [14] R. Engel, astro-ph/9811225.
  - [15] T. Sjostrand *et al.*, *Comput. Phys. Commun.* **135**, 238 (2001); T. Sjostrand *et al.*, hep-ph/0108264.
  - [16] S. Razzaque *et al.*, (to be published).
  - [17] E. Waxman and J.N. Bahcall, *Phys. Rev. D* **59**, 023002 (1999).
  - [18] F. Halzen and D. Hooper, *Rep. Prog. Phys.* **65**, 1025 (2002); RICE Collaboration, I. Kravchenko *et al.*, *Astropart. Phys.* **19**, 15 (2003); astro-ph/0206371; P. Gorham, in *Ultra high Energy Particles from Space*, Aspen (2002).